SCIENCE CHINA
Technological Sciences

• LETTER •

October 2025, Vol. 68, Iss. 10, 2080201:1–2080201:2
https://doi.org/10.1007/s11431-025-3003-2

A new topology optimization method of an asymmetric phononic crystal for enhancing bandgap distributions

Liming GUO[1,2], Chiye YANG[1,2], Jing LIU[1,2*], Hengtai NI[1,2], Guang PAN[1,2] & Baowei SONG[1,2]

[1] *School of Marine Science and Technology, Northwestern Polytechnical University, Xi'an 710072, China*
[2] *Key Laboratory for Unmanned Underwater Vehicle, Northwestern Polytechnical University, Xi'an 710072, China*

Received March 18, 2025; accepted August 4, 2025; published online September 10, 2025

Citation: Guo L M, Yang C Y, Liu J, et al. A new topology optimization method of an asymmetric phononic crystal for enhancing bandgap distributions. Sci China Tech Sci, 2025, 68(10): 2080201, https://doi.org/10.1007/s11431-025-3003-2

To address the challenges for vibration suppression in the precision sensors of underwater vehicles, phononic crystals have attracted significant attention due to the superior capabilities in elastic wave manipulation and vibration suppression. Unlike conventional damping materials, the phononic crystals can effectively suppress the wave propagation in the specific frequency ranges due to the unique periodic microstructures. Through topology optimization methodologies, the microstructure of phononic crystals can be systematically designed, which significantly enhances the characteristics of band gaps in the low frequency and width [1–4]. However, the current works mainly focused on the phononic crystal designs with symmetric constraints, which limits the development in this field. Therefore, the asymmetric designs for optimizing the bandgap distribution can provide some novel insights for the phononic crystal innovations.

In this paper, the symmetry constraints of phononic crystal design are removed to explore the novel solutions. The plane wave expansion method is employed to establish the model of a phononic crystal. The dispersion relations and bandgap distributions are discussed. The topological structures of phononic crystals are optimized through genetic algorithms to obtain the widest bandgap distributions in the first 6 bands. The results demonstrate that the asymmetric phononic crystals exhibit various patterns, and the vibration suppression range is improved to 141.71% by systematically introducing these multiple phononic crystals.

Figure 1(a) demonstrates the schematic of unit cells with symmetrical and asymmetrical characteristics, where the yellow and blue areas represent the aluminum and epoxy resin, respectively. The lattice constant of the unit cell is $a = 50$ mm. The unit cell of a phononic crystal is discretized into multiple subregions, where each subregion is assigned a specific material. The material distributions of the whole unit cell can be represented by an array X, where 0 denotes the epoxy resin and 1 denotes the aluminum. In this way, the value of X corresponds to the structural topology, as illustrated in Figure 1(b) and (c). The plane wave expansion method is employed to calculate the band gaps of a phononic crystal. Generally, the bandgap formation of in-plane waves in the two-dimensional structures is a challenging problem. Therefore, this work mainly focuses on the band gaps of in-plane waves.

For the in-plane waves propagating through the solid structures, the governing equations are [5]

$$
\begin{aligned}
\rho(\mathbf{r})\frac{\partial^2 u_x}{\partial t^2} &= \frac{\partial}{\partial x}\left[\lambda(\mathbf{r})\left(\frac{\partial u_x}{\partial x}+\frac{\partial u_y}{\partial y}\right)+2\mu(\mathbf{r})\frac{\partial u_x}{\partial x}\right]+\frac{\partial}{\partial y}\left[\mu(\mathbf{r})\left(\frac{\partial u_x}{\partial y}+\frac{\partial u_y}{\partial x}\right)\right],\\
\rho(\mathbf{r})\frac{\partial^2 u_y}{\partial t^2} &= \frac{\partial}{\partial x}\left[\mu(\mathbf{r})\left(\frac{\partial u_y}{\partial x}+\frac{\partial u_x}{\partial y}\right)\right]+\frac{\partial}{\partial y}\left[\lambda(\mathbf{r})\left(\frac{\partial u_x}{\partial x}+\frac{\partial u_y}{\partial y}\right)+2\mu(\mathbf{r})\frac{\partial u_y}{\partial y}\right],
\end{aligned}
\tag{1}
$$

where $\mathbf{r}$ is the position vector, λ and μ are the Lamé parameters, and u_x and u_y are the components of the displacement $\mathbf{u}$ along the x and y directions, respectively.

Due to the periodic nature of the metamaterial, eq. (1) can be derived by applying Bloch's theorem and the Fourier series expansion of coefficients, the resulting expression is

$$
\begin{aligned}
&\omega^2\sum_G \rho(\mathbf{G}''-\mathbf{G})\mathbf{u}_k^x(\mathbf{G})\\
&=\sum_G\Big[\lambda(\mathbf{G}''-\mathbf{G})(\mathbf{k}+\mathbf{G})_x(\mathbf{k}+\mathbf{G}'')_x+\mu(\mathbf{G}''-\mathbf{G})(\mathbf{k}+\mathbf{G})_y(\mathbf{k}+\mathbf{G}'')_y\\
&\quad+2\mu(\mathbf{G}''-\mathbf{G})(\mathbf{k}+\mathbf{G})_x(\mathbf{k}+\mathbf{G}'')_x\Big]\cdot\mathbf{u}_k^x(\mathbf{G})\\
&\quad+\sum_G\Big[\lambda(\mathbf{G}''-\mathbf{G})(\mathbf{k}+\mathbf{G})_y(\mathbf{k}+\mathbf{G}'')_x+\mu(\mathbf{G}''-\mathbf{G})(\mathbf{k}+\mathbf{G})_x(\mathbf{k}+\mathbf{G}'')_y\Big]\cdot\mathbf{u}_k^y(\mathbf{G}),\\
&\omega^2\sum_G \rho(\mathbf{G}''-\mathbf{G})\mathbf{u}_k^y(\mathbf{G})\\
&=\sum_G\Big[\lambda(\mathbf{G}''-\mathbf{G})(\mathbf{k}+\mathbf{G})_y(\mathbf{k}+\mathbf{G}'')_y+\mu(\mathbf{G}''-\mathbf{G})(\mathbf{k}+\mathbf{G})_x(\mathbf{k}+\mathbf{G}'')_x\\
&\quad+2\mu(\mathbf{G}''-\mathbf{G})(\mathbf{k}+\mathbf{G})_y(\mathbf{k}+\mathbf{G}'')_y\Big]\cdot\mathbf{u}_k^y(\mathbf{G})\\
&\quad+\sum_G\Big[\lambda(\mathbf{G}''-\mathbf{G})(\mathbf{k}+\mathbf{G})_x(\mathbf{k}+\mathbf{G}'')_y+\mu(\mathbf{G}''-\mathbf{G})(\mathbf{k}+\mathbf{G})_y(\mathbf{k}+\mathbf{G}'')_x\Big]\cdot\mathbf{u}_k^x(\mathbf{G}),
\end{aligned}
\tag{2}
$$

* Corresponding author (email: jliu0922@nwpu.edu.cn)

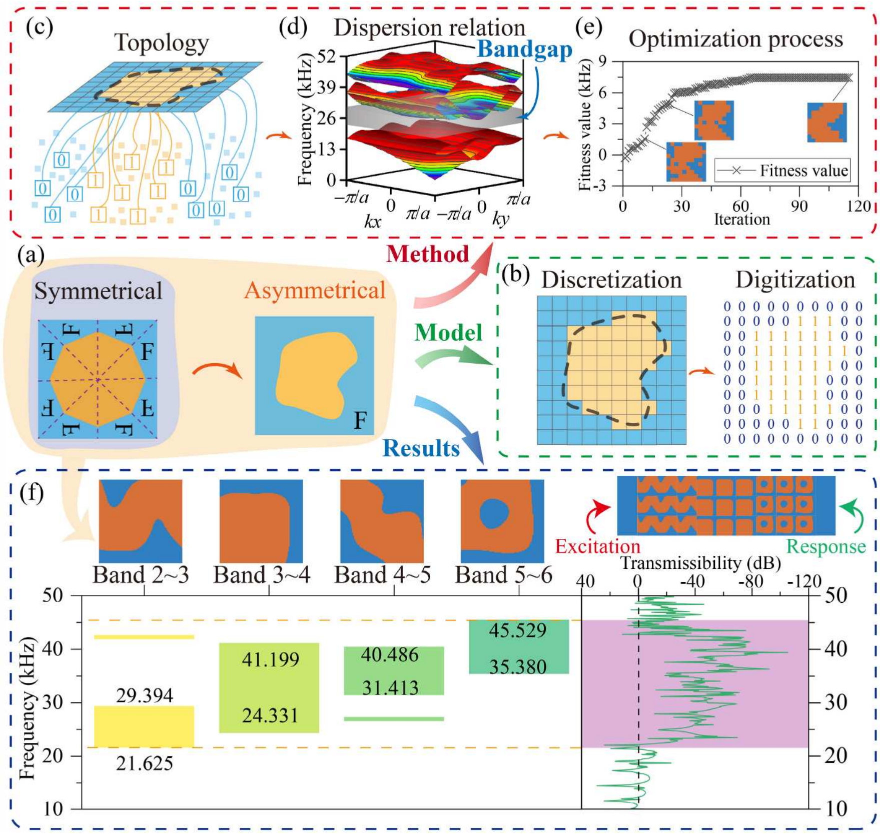

Figure 1 (a) Asymmetric phononic crystal structural layout; (b) discretized representation of material distributions; (c) the topological structures and design space; (d) dispersion characteristics and bandgap distributions of phononic crystal; (e) topology optimization design process; (f) the designs of phononic crystals and corresponding bandgaps.

where **G** and **G**″ are vectors in the reciprocal space. The detailed derivation process can be found in ref. [6]. By solving the eigenvalue of eq. (2), the band diagrams and the band gaps are identified, as shown in Figure 1(d).

To obtain the widest width of band gaps between adjacent bands, the genetic algorithm is employed to perform the topology optimization of the metamaterial, as shown in Figure 1(e). The objective function is

$$Fval = \min\left(\omega_{i+1}(X,\mathbf{k})\right) - \max\left(\omega_i(X,\mathbf{k})\right),\ (i = 1, 2, \cdots, 5), \tag{3}$$

where ω_i is the angular frequency of the ith band, and X denotes the material distribution in the unit cell. The introduction of asymmetric design increases the number of optimization parameters. To address this issue, the material-field series-expansion method is employed in this study [7]. The size of observation points is 50×50, the size of the discretized unit cell is 100×100, and the correlation length is 0.3a.

The widest band gaps in the first six bands are investigated. As shown in Figure 1(f), the band gaps are opened in bands 2–6 with various patterns. The frequency range of the bandgap in bands 2–3 is 21.625–29.394 kHz. The aluminum is distributed in a wavy pattern. The frequency range of the bandgap in bands 3–4 is 24.331–41.199 kHz. The shape is distributed in a square pattern. The frequency range of bandgaps in bands 4–5 is 31.413–40.486 kHz; and the frequency range of the bandgap in bands 5–6 is 35.38–45.529 kHz. Figure 1(f) illustrates the distributions of bandgaps and the corresponding topological structures. The widest single bandgap is between bands 3–4, whose width is 16.868 kHz. Moreover, the vibration transmissibility of a planar plane with multiple systematically distributed phononic crystals is analyzed. The vibration suppression range corresponds to the bandgap regions, which demonstrates the existence of the band gaps and the effectiveness of the optimization method. The vibration suppression frequency range reaches 141.71% of the single bandgap width.

Acknowledgements This work was supported by the National Key Research and Development Programme of China (Grant No. 2023YFB3406302), the National Natural Science Foundation of China (Grant No. 52175120), and Key Research, Development Plan of Shaanxi (Grant No. 2024GH-ZDXM-29).

References

1 Sigmund O, Søndergaard J J. Systematic design of phononic band-gap materials and structures by topology optimization. Philos Trans R Soc London Ser A-Math Phys Eng Sci, 2003, 361: 1001–1019
2 Bilal O R, Hussein M I. Ultrawide phononic band gap for combined in-plane and out-of-plane waves. Phys Rev E, 2011, 84: 065701
3 Xiong C, Lee C Y, Qin Q H. Topology optimization of single-phase phononic crystals based on a search-space-reduction strategy with a Genetic Algorithm. Mater Today Commun, 2023, 34: 105069
4 Yan G, Yao S, Li Y, et al. Topological optimization of thin elastic metamaterial plates for ultrawide flexural vibration bandgaps. Int J Mech Sci, 2023, 242: 108014
5 Guo L, Liu J, Gao N, et al. Wave propagation behaviors of a low-symmetry reentrant chiral structure with mass inclusion in a single material. Eur J Mech-A Solids, 2023, 99: 104951
6 Xie L, Xia B, Liu J, et al. An improved fast plane wave expansion method for topology optimization of phononic crystals. Int J Mech Sci, 2017, 120: 171–181
7 Luo Y, Bao J. A material-field series-expansion method for topology optimization of continuum structures. Comput Struct, 2019, 225: 106122